A Fourier transform telescope for sub-arcsecond imaging of X-rays and gamma rays

C. J. Crannell*, G. J. Hurford**, L. E. Orwig* and T. A. Prince**
*Laboratory for Astronomy and Solar Physics, NASA/GSFC,
Greenbelt MD 20771
**California Institute of Technology,
Pasadena CA 91125

Abstract

This paper describes a Fourier transform telescope designed to image solar flare X-rays and gamma rays at energies up to 1 MeV with arcsecond or subarcsecond resolution. The imaging technique makes use of a bigrid collimator divided into a number of smaller areas called subcollimators. The grids in each subcollimator consist of a set of linear apertures so configured that each subcollimator provides a measurement of a single Fourier component of the angular distribution of the source. The imaging concept is therefore a mathematical analog to aperture synthesis in radio astronomy. For X-ray and gamma-ray astronomy, this approach has significant advantages in terms of relaxed requirements for position sensitivity in the detector and for control of grid alignment in the large scale telescope structure. The concept of the Fourier transform telescope will be illustrated with numerical parameters of a version now under study for the Pinhole/Occulter Facility.

Introduction

Observations of solar flares provide an opportunity to study nearby examples of energy release and particle acceleration processes that occur on many scales in astronomy. Accelerated electrons, which play a crucial role in the energetics of solar flares, can be directly detected through their microwave, hard X-ray and gamma-ray emission. For microwaves, such emission is due to the interaction of the electrons with the ambient magnetic field. For hard X-rays and continuum gamma rays, it is due to Coulomb collisions.

The spectral and temporal characteristics of such emission have been studied extensively with ground-based and satellite instrumentation for over 20 years. For most of this period, interpretation of these data has been hampered by an inability to image the sources so as to locate the energetic electrons in their physical context on the Sun. It is only during the most recent solar maximum that microwave imaging has achieved the arcsecond resolution required to resolve the radio sources.[1,2] Although hard X-ray sources are expected to be at least as compact, the resolution and sensitivity achieved to date by hard X-ray telescopes have lagged well behind that available at radio wavelengths. Because of the different emission and propagation mechanisms, imaging of both microwaves and the hard X-ray/gamma-ray continuum is needed to understand the acceleration and dynamics of the energetic electrons.

Despite limitations, results obtained with the hard X-ray imaging instruments during the recent solar maximum have suggested the potential of such observations to answer fundamental questions on the nature of solar flares. In particular, the Hard X-ray Imaging Spectrometer (HXIS) on the Solar Maximum Mission and the Solar Hard X-ray Telescope on the Japanese Hinotori spacecraft demonstrated that hard X-rays, with energies up to 40 keV, appear to come from the footpoints of flaring magnetic loops.[3,4] This result has been used to argue that the X-rays must be produced by beams of high-energy electrons incident on the thick target of the lower solar corona and chromosphere (Figure 1). An alternative interpretation of the limited imaging information, namely that most of the X-rays may come from a more diffuse region around and between the footpoints, cannot be ruled out. The limited angular resolution (≥8 arcseconds) has precluded effective discrimination between electrons which propagate immediately to the footpoints and those which are well trapped in the magnetic mirror formed by the flaring loops. Comparisons of microwave and hard X-ray imaging data are further frustrated by the total absence of any X-ray imaging at energies above 100 keV, whereas it is electrons at these energies that provide the bulk of microwave emission.

The X-ray telescope parameters that must be improved are energy range, sensitivity, time resolution and angular resolution. Imaging well above 100 keV is necessary so that hard X-ray images can be compared directly with microwaves. Sensitivity and time resolution must be increased so that the simultaneity of footpoint brightenings can be established with a precision better than the few tenths of a second travel time for electrons traversing a typical flaring loop. Angular resolution of better than 1 arcsecond is needed to fully resolve the bright patches and to determine the

distribution of emission from the different parts of the magnetic arches. Finally, the dynamic range must be sufficient to produce high-contrast images, since the emission from footpoints may be a factor of 10 or more brighter than the emission from the tops of loops.

Efforts are underway to develop hard X-ray and gamma-ray instrumentation with the required capabilities. The purpose of this paper is to describe progress made on the development of such techniques, whose successful application will greatly enhance our understanding of particle acceleration and propagation in solar flares.

In the next section we describe an imaging technique which is capable of achieving the instrumental requirements outlined above. In the final section, an instrument configuration appropriate for flight on the Shuttle and some prototype components are described.

Imaging technique

For photon energies above a few keV, the use of reflecting or refracting optics is not possible. Therefore hard X-ray imaging techniques are restricted to collimation schemes. The choice is further constrained since sensitivity and angular resolution requirements rule out such conceptually simple techniques as lead-pipe or slat collimators. For high sensitivity, modern implementations of the multiple pinhole camera using uniformly redundant arrays are attractive.[5] Their disadvantage, however, is that to achieve high angular resolution, they require either detectors with high spatial resolution, (comparable to that of apertures in the mask) or excessively large separation of mask and detector. At present, this appears to preclude imaging at the arcsecond level.

One X-ray imaging technique extensively used in the past to achieve high resolution is based on the bigrid collimator.[6] The collimator for such telescopes consists of a pair of well-separated grids with linear apertures and a detector (without spatial resolution) located behind the rear grid. The collimator is mechanically rocked or rotated[7] to modulate the detected X-ray flux. Such telescopes are well suited to the detection and location of weak, pointlike sources.

Imaging capabilities can be improved by the use of additional intermediate grids. The

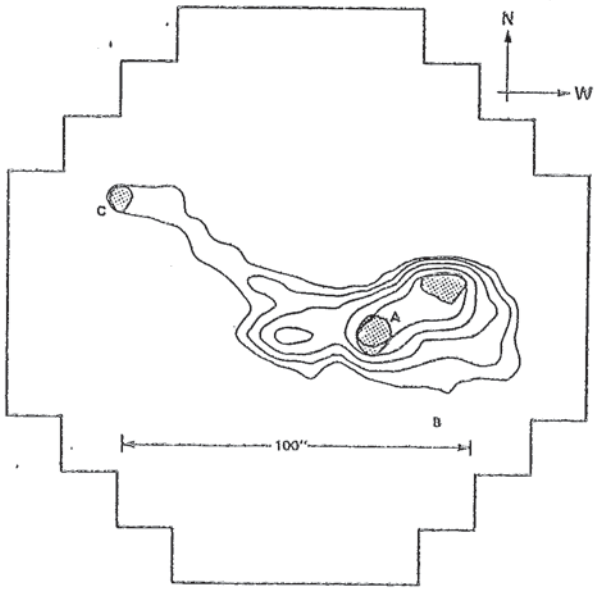

Figure 1. Contour plot of an X-ray image obtained with HXIS for a flare that occurred on November 5, 1980. The contours show the intensity of the X-ray emission in the energy range from 3.5 to 8 keV. The three cross-hatched regions marked A, B, and C show the location of the brightest emission in the energy range from 16 to 30 keV. The exposure time for the image was 13.5 seconds during the most intense part of the hard X-ray flare. The image suggests the simultaneous brightening of loop footpoints separated by 70,000 km. The brightenings occurred within 10 seconds of each other so that only signals travelling between the footpoints with velocities close to the speed of light could give the observed simultaneity. (after reference 16)

HXIS experiment, discussed above, used a 10 grid collimator and ~10^3 small, individual detectors to achieve 8 arcsecond imaging.[8] The extension of multigrid collimators to achieve higher resolution for solar applications leads, however, to stringent requirements for a metering structure to maintain alignment of the grids.[9]

The most promising approach for high-resolution, high-sensitivity imaging at hard X-ray and gamma-ray energies is based on a fresh perspective on the old idea of the bigrid imaging collimator.[6] The imaging collimator differs from the modulation collimator in that the top and bottom grids have a slightly different pitch. In this case, the modulation is spatial rather than temporal. A point source viewed by such a collimator has a count rate distribution with an approximately triangular profile on a spatial scale coarse compared to the aperture size. (Figure 2)

Since this spatial modulation can be measured with a detector whose spatial resolution need not be comparable to the aperture width, the angular resolution limitations associated with the scatter-hole camera are overcome. The use of spatial rather than temporal modulation also eliminates the possibility of misinterpreting rapid temporal variations in the incident X-ray flux in terms of modulation, and helps to enhance the dynamic range by minimizing such detrimental factors as pulse pileup during intense bursts.

We now consider the key feature of the bigrid collimator for our present purpose. As was suggested by Makishima et al.[10] and subsequently demonstrated formally,[11] if one considers only the principle spatial Fourier component of the modulation, then its amplitude and phase measures a specific Fourier component of the angular distribution of the source. Although achieved by a physically different process, this is in precise mathematical analogy to the correlated output of a single baseline in radio interferometry. In the radio domain, interferometers such as the VLA achieve imaging by using many baselines to measure many Fourier components of the source, and then performing the inverse Fourier transform. For hard X-ray imaging, a corresponding set of Fourier components is measured by a set of subcollimators with an appropriate range of aperture widths and orientations, and then the image created by the same Fourier inversion process. Simulations have shown that many of the image processing techniques, highly developed for the radio interferometry application,[12] can be carried over to the X-ray domain.

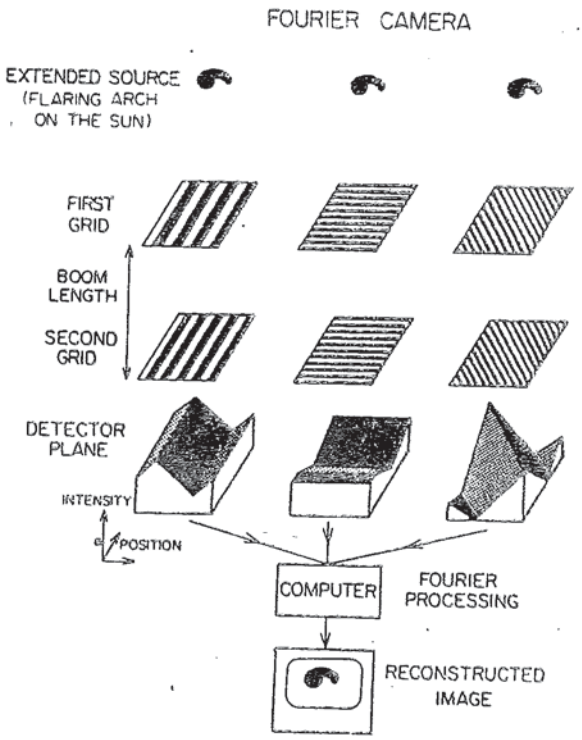

Figure 2. Schematic illustration of a Fourier transform telescope showing 3 subcollimators, each consisting of a pair of well separated grids, and a detector behind the rear grid. The different grid aperture sizes and orientations measure different Fourier components of the extended source distribution.

We now discuss the implications of this imaging technique for telescope design, and then review some differences with the radio interferometry analog. Consider a bigrid collimator with aperture widths, ~w; detector resolution, S; subcollimator diameter, D; and grid separation, L. We require that w << S << D << L. On the sky, the spatial period of the Fourier component measured by a subcollimator is given by 2w/L, while the position angle of the component is determined by the aperture orientation. The field of view is given by D/L.

What are the structural implications of imaging at the arcsecond or subarcsecond level? First, we note three obvious but significant points: a bigrid collimator has no intermediate grids to consider; relative displacements of the top and bottom grids parallel to the linear apertures have no effect on instrument response; and imaging is quite insensitive to variations in the grid separation, L, or to grid rotation about axes orthogonal to the telescope axis.

More noteworthy is that grid displacements† orthogonal to the apertures do not decrease the amplitude of the spatially modulated count rate distribution. They do shift the location of the maximum so that such displacements directly affect the measured phase of the Fourier component. To compensate for this, it is necessary to have knowledge of the relative grid positions to an angular precision good compared to w/L, that is, compared to the angular resolution. Provided that detected counts can be associated with post facto measurements of this displacement, it is NOT necessary to control the grid displacement to such a high level of precision. The requirement of knowledge, as distinct from control, of small scale displacements or the large-scale telescope structure is the key to the practicality of high-resolution imaging at these wavelengths.

The remaining alignment component, namely relative rotation or twist of the upper and lower grids, must be controlled so that the apertures remain parallel. The tolerance here, however, is determined by w/D, not w/L. If the detector spatial resolution, S, is two-dimensional this tolerance can be further relaxed to the order of w/S.

Apart from twist, the most significant control requirement on the large scale telescope structure is set by the field of view which is given by D/L.

In summary, Fourier transform imaging of hard X-rays and gamma rays is a technique whose angular resolution is not limited by either detector resolution or large scale structural stability requirements. Rather the factors which fundamentally limit its potential resolution are: X-ray diffraction by the grid apertures;[13] the minimum width of apertures which can be fabricated in material which is opaque at photon energies of interest; the maximum achievable separation of the grid planes; and the availability of optical aspect systems of corresponding resolution.

The optical design of such a Fourier transform X-ray telescope presents an interesting contrast to that of a radio interferometer. At a given radio wavelength, the field of view and sampled Fourier component are determined by the antenna diameters and relative antenna locations respectively. For an interferometer consisting of N antennas, up to N(N-1)/2 Fourier components can be simultaneously measured. The choice of these components, however, is not independent since they are determined by the locations of only (N-1) antennas. In the X-ray case, the N Fourier components measured by N subcollimators can each be chosen independently.

For stable sources, radio interferometers often make use of earth rotation synthesis whereby successive measurements taken during the day enables each baseline to measure many Fourier components. The corresponding advantage (orbital rotation synthesis?) is available in the X-ray domain by rotating the telescope at a convenient rate.

For spectroscopy over a wide range of wavelengths, radio interferometry has the weakness that the Fourier component sampled by a given baseline varies inversely with wavelength. Thus a given interferometer will be sensitive to structure of different size scales at different wavelengths. In the case of X-ray imaging, simultaneous measurements of the same Fourier component at different frequencies are limited only by the energy range of the detector. Thus X-rays from energies below 10 keV (which delineate the thermal component of the flaring plasma) through gamma rays can be imaged simultaneously with a common set of optics.

Telescope Development Status

The Fourier transform imaging technique outlined above can be adapted to achieve high

† Displacement in this context means the direction of the vector between reference points on the two grids relative to the vector from the telescope to the source.

angular resolution, sensitivity, and energy range for a wide range of flight opportunities, limited primarily by the size of the instrument payload that can be carried on the mission. One of the earliest versions is expected to fly on the Japanese HESP satellite, scheduled for launch in 1991. This configuration, with a total boom length of ~1 m will achieve an angular resolution of ~6 arcseconds, up to ~100 keV.

The most ambitious configuration considered to date would fly first as part of the shuttle-based Pinhole/Occulter Facility (P/OF) [14] and then as part of the Advanced Solar Observatory which is being studied as a facility for Space Station. With apertures as small as 50 microns, and a 50 m boom separating the grids, spatial resolution of 0.2 arcseconds would be achievable. The shuttle-based P/OF (Figure 3) would also support advanced coronagraph instrumentation and a multiple-pinhole X-ray camera. Although the latter would have lower resolution than the Fourier transform telescope, it would be able to image more complex sources than could a Fourier transform telescope with a limited number of subcollimators.

A third configuration which has been studied is appropriate to free-flying satellites of the MMS or Explorer class. Equipped with a 7 m boom and occupying a 1 x 1 m area, such a telescope could achieve 1.4 arcsecond resolution. The subcollimators would have dimensions of ~10 x 10 cm, a configuration that has the merit of a 50 arcminute field of view, thereby allowing continuous full Sun observations.

A detector resolution of 1 cm is quite adequate for these configurations. Such resolution is readily achievable with good detection sensitivity using proportional chambers for energies up to ~50 keV. Recent developments of NaI scintillation cameras for balloon applications can extend the required detector capability up to at least 1 MeV.[15] The energy range of the optimal response of the NaI scintillation cameras can be chosen by varying the thickness of the NaI and the number, size, and shape of the photomultiplier tubes. In general, a thick (5 cm) NaI detector has good sensitivity for energies up to 1 Mev at the expense of somewhat poorer resolution (~1.5 cm) for energies below 100 keV. A thinner (<2 cm) NaI detector provides good position resolution down to 50 keV with lower sensitivity above 500 keV.

The extension of imaging to higher energies also requires grids that are opaque to the higher energy photons. For instance, tungsten grids of about 4 mm thickness are required to achieve one attenuation length at 500 keV. For coarse grids of the required thickness, conventional machining techniques can be used (Figure 4). Since direct machining is not

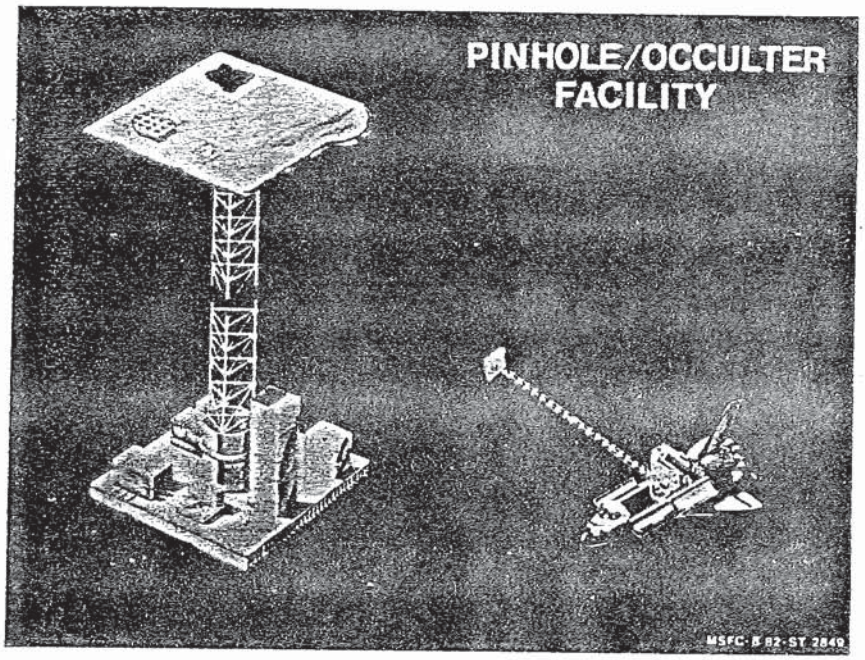

Figure 3. Illustration of the Pinhole/Occulter Facility. The front grid of the Fourier transform telescope is in the left corner of the mask located at the end of a 50 m boom. The other grid and detectors are mounted on the detector plane on the IPS pointing system in the shuttle bay.

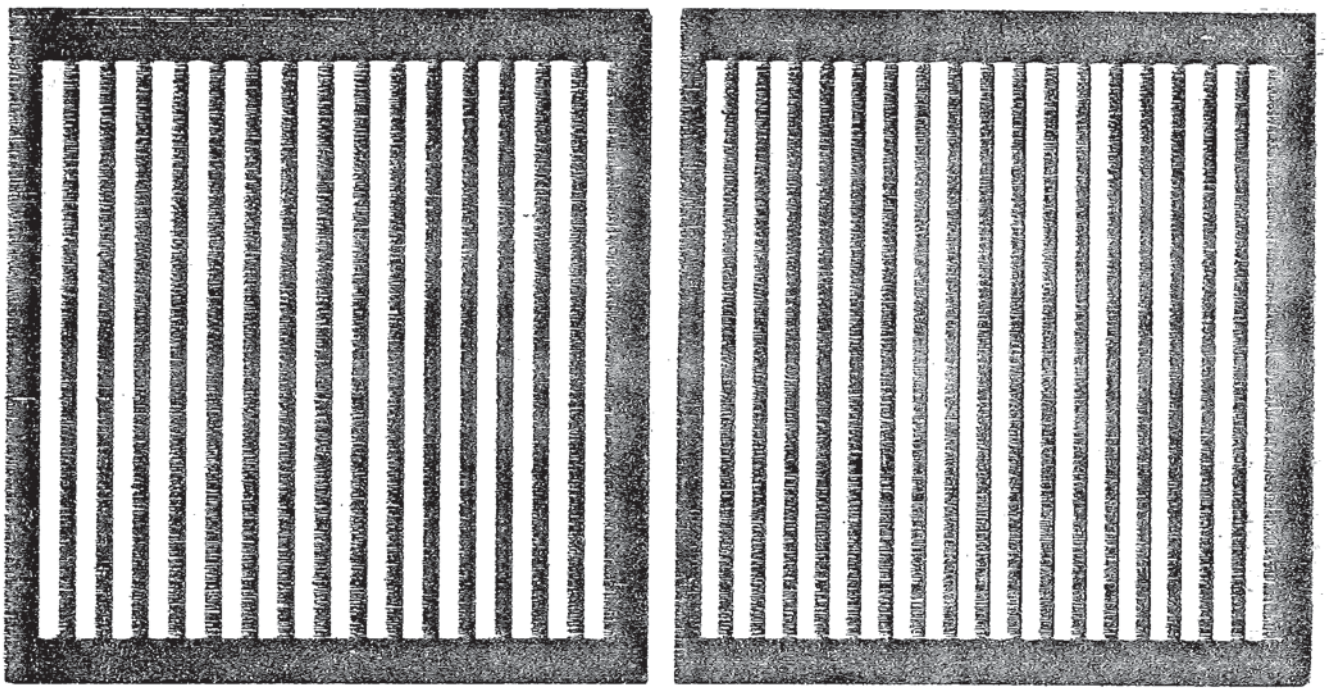

Figure 4. A prototype pair of coarse grids, each machined from a solid block of tungsten using an ELOX machine. The dimensions of the slatted portion are 10 x 10 x 1 cm. The slat thicknesses are 0.625 cm and 0.556 cm respectively. The reader is invited to make copies of this figure on a transparency, cut out and then superpose the 16- and 18-pair grids. The resulting Moire patterns will illustrate the sensitivity of a low resolution detector to small shifts in position (or incident angle in the case of well separated grids).

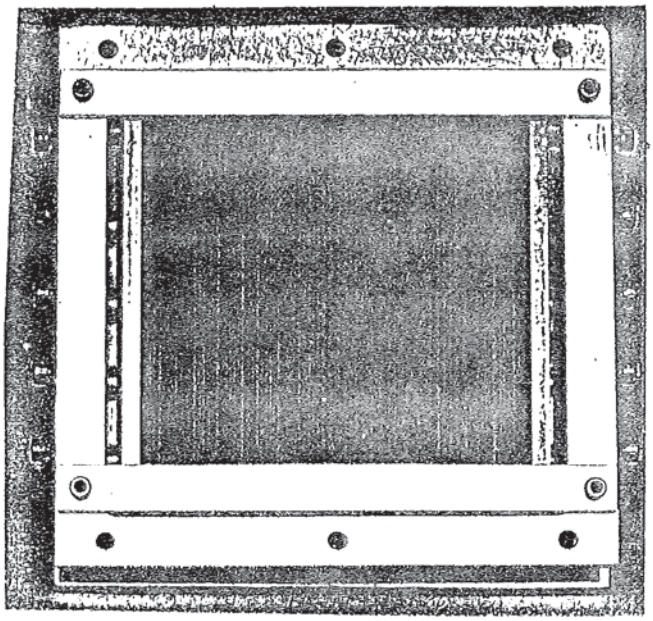

Figure 5. Photograph of a prototype fine grid collimator assembly, showing the alternating tantalum slats and mylar spacers. The steel bars and screws on either side of the stack are used to compress and align the tantalum/mylar stack within the frame. The overall stack dimensions are 10 x 10 x 0.5 cm and the individual tantalum and mylar slats are nominally 100 microns thick. The large scale features are due to variations in width, not thickness of the slats.

feasible for the finer grids, two alternate approaches can be taken to achieve thick grids with apertures as small as 50 microns. The first approach employs thin tungsten foils which have been etched to form the desired grid pattern. Large numbers of such foils are then stacked to achieve the desired thickness. Japanese workers have successfully fabricated Cu-Be grids with feature size of 70 microns to a thickness of ~1 cm using this technique.

The second approach employs alternating strips of high-Z (e.g. tungsten or tantalum) and low-Z (e.g. mylar) materials. This technique has the disadvantage that even the mylar severely attenuates X-rays of the lowest energies in which we ere interested. It has the advantage, however, of simplicity and low cost.

Investigating this second approach at GSFC, an initial pair of fine (100 microns) collimator grids has been fabricated and has undergone preliminary performance tests. Each grid was made by compressing alternate strips of tantalum and mylar inside a rigid aluminum frame using screw-adjustable pressure plates. A photograph of one of the completed units is shown in Figure 5. Prototype top and bottom grids were fabricated with 500 and 502 mylar "apertures" respectively within the 10-cm collimator length. To minimize systematic errors, the tantalum and mylar slats for both fine-grid assemblies were cut from the same sheets of raw material. The RMS deviation in the paired thickness was measured to be less than 3 microns. Cumulative errors were consistent with the expected random walk fluctuations. Since material tolerances much finer than 3 microns can be readily obtained, we are confident that a version of this fabrication technique would yield high-angular resolution grids suitable for use in the Fourier-transform collimator system.

In summary, we feel that the imaging concept represented by the Fourier transform telescope, coupled with advances in grid and detector technology has reached the point where astronomical imaging with arcsecond and subarcsecond resolution can be achieved in the hard X-ray and gamma-ray regime.

Acknowledgements

The imaging techniques described here have been stimulated by contributions from a large number of individuals throughout the high-energy solar physics and astrophysics community. Extensive discussion and review has come from NASA working groups and study teams, namely the Hard X-ray Imaging Facility Definition Team under L. E. Peterson, the Pinhole/Occulter Facility Science Working Group under H. R. Hudson and E. Tandberg-Hanssen, the MAX '91 Science Study Committee under B. R. Dennis, and the High-Energy Facility Workshop for the Advanced Solar Observatory under E. P. Chupp. At Caltech this work is supported by NSF grant ATM-83-09955 and NASA grant NGR 05-002-160.

References

1. Kundu, M. R. and Vlahos, L., Space Science Reviews, 32, 405. 1982.
2. Marsh, K. A. and Hurford, G. J., Ann. Rev. Astron. Astrophys. 20, 497. 1982.
3. Duijveman, A., Hoyng, P., and Machado, M. E., Solar Phys., 81, 137. 1982.
4. Tsuneta, S., Proc. Japan-France Seminar on Active Phenomena in the Outer Atmosphere of the Sun and Stars, 3-7 October 1983, (J. -C. Pecker and Y. Uchida, eds.) CNRS and Observatoire de Paris, p.243. 1983.
5. Fenimore, E. E. and Cannon, T. M., Appl. Optics, 17, 337. 1978.
6. Bradt, and 6 co-authors, Space Science Reviews, 8, 471. 1968.
7. Schnopper, H. W. and Thompson, R. I., Space Science Reviews, 8, 534. 1968.
8. van Beek, H. F., Hoyng, P., Lafleur, B. and Simnett, G. M., Solar Phys., 65, 39. 1980.
9. Hurford, G. J., Proc. SPIE 106, 163, 1977.
10. Makishima, K. and 6 co-authors, in van der Hucht, K. and Vaiana, G. S. (eds.), New Instrumentation for Space Astronomy (New York: Pergammon), p277. 1977.
11. Hurford, G. J. and Hudson, H. S., BBSO preprint 0188. 1979.
12. Synthesis Mapping: Proceedings of the NRAO-VLA Workshop held at Socorro, New Mexico, June 1982, Thompson, A. R. and D'Addario, L. R. (eds.) 1982.
13. Lindsey, C. E., J. Opt. Soc. Am., 68, 1708. 1978.
14. Cook, W. R., Finger, M. and Prince, T. A., IEEE Trans. in Nucl. Sci., NS-31, 348. 1984.
15. NASA Technical Paper 2168. 1983.
16. Dennis, B. R. Solar Phys., 100, (in press). 1985.